LETTERS
PUBLISHED ONLINE: 9 DECEMBER 2012 | DOI: 10.1038/NCLIMATE1760
nature climate change

Dolomite-rich coralline algae in reefs resist dissolution in acidified conditions

M. C. Nash[1]*, B. N. Opdyke[2], U. Troitzsch[2], B. D. Russell[3], W. H. Adey[4], A. Kato[5], G. Diaz-Pulido[6], C. Brent[2], M. Gardner[2], J. Prichard[2] and D. I. Kline[7,8]

Coral reef ecosystems develop best in high-flow environments but their fragile frameworks are also vulnerable to high wave energy. Wave-resistant algal rims, predominantly made up of the crustose coralline algae (CCA) *Porolithon onkodes* and *P. pachydermum*[1,2], are therefore critical structural elements for the survival of many shallow coral reefs. Concerns are growing about the susceptibility of CCA to ocean acidification because CCA Mg-calcite skeletons are more susceptible to dissolution under low pH conditions than coral aragonite skeletons[3]. However, the recent discovery[4] of dolomite ($Mg_{0.5}Ca_{0.5}(CO_3)$), a stable carbonate[5], in *P. onkodes* cells necessitates a reappraisal of the impacts of ocean acidification on these CCA. Here we show, using a dissolution experiment, that dried dolomite-rich CCA have 6–10 times lower rates of dissolution than predominantly Mg-calcite CCA in both high-CO_2 (~700 ppm) and control (~380 ppm) environments, respectively. We reveal this stabilizing mechanism to be a combination of reduced porosity due to dolomite infilling and selective dissolution of other carbonate minerals. Physical break-up proceeds by dissolution of Mg-calcite walls until the dolomitized cell eventually drops out intact. Dolomite-rich CCA frameworks are common in shallow coral reefs globally and our results suggest that it is likely that they will continue to provide protection and stability for coral reef frameworks as CO_2 rises.

Coralline algae form extensive carbonate structures on the high-energy windward side of many tropical coral reefs. For example, the algal rim on the fringing reef of Rodrigues Island (Indian Ocean) is ~11 km long, 4 m thick and in parts protrudes ~1m above the reef flat[6], providing substantial protection for island communities from high-energy waves. Only the surface veneer (the top few millimetres) of CCA is living[7] and the dense carbonate underneath the algal rim is predominantly *in situ* CCA skeleton and overlapping layers of coral branches cemented together by CCA crusts[6]. Development of these reef structures is dependent on preservation of the dead CCA skeleton post-mortem. Thus, understanding how declining seawater pH will affect this skeletal preservation is of paramount importance if we are to understand the changes to coral reef structural stability in a high-CO_2 world.

In the 1950s–1970s the mineral composition of coralline algae skeletons was determined to be ~12–18 mol% Mg-calcite[8–10]. However, many bulk chemical analyses of tropical coralline algae showed a surplus of magnesium compared with those determined by X-ray diffraction (XRD) using Mg-calcite peak position[8,9]. Recently, we discovered this discrepancy was due to the presence of previously undetected dolomite and magnesite ($MgCO_3$) forming within the cell spaces[4]. Past determinations of thermodynamic solubility for coralline algae were based on the assumption that they were composed of Mg-calcite[10–12]. As dolomite was not believed to form in the modern marine environment, determining dolomite solubility under these conditions was considered of limited importance[12]. Dolomite stability has been inferred from the geologic record with a noted correlation between dolomite abundance and periods of higher CO_2 (lower CO_3 saturation state) in the Phanerozoic eon[5] indicating dolomite stability under lower pH conditions.

We carried out dissolution experiments on fragments (~1 cm^3) of CCA (*P. onkodes*) collected fresh, then dried, from the Heron Island reef front (Great Barrier Reef, Australia) and exposed to ambient sea water as a control and an enriched CO_2 treatment (Methods). pH (National Bureau of Standards scale) ranged from 7.85 to 8.55 (control) and 7.69–8.44 (treatment) tracking natural diurnal changes measured in the lagoon water[13] (Supplementary Tables S1–S3 and Figs S1 and S2). Weight changes from experiments using living CCA are a combination of growth processes and skeletal dissolution[14]. Previous dissolution experiments have used dried, powdered CCA (refs 10,11), in beakers, with pH conditions not representative of the coral reef environment. The aim of this experiment was to determine the relationship between the mol% $MgCO_3$ of the CCA skeleton and dissolution without the influence of living processes. Although it was necessary to dry the CCA until dead, the crusts were kept intact so as to obtain results most closely replicating dissolution of exposed skeleton in the natural environment. Understanding this non-biotic dissolution process is important because when the CCA skeleton is exposed in the reef, for example by bio-erosion or breakages, then, without the protection of organic membranes, dissolution will be constrained by the skeletal composition (mineral and structural)[12].

Considering the prevailing theories that Mg-calcites with higher Mg content will undergo greatest dissolution, we were surprised to find a trend in the opposite direction (Fig. 1a). After ten days in the control and CO_2 treatments, coralline algae from the higher mol% group (17.27 – 18 mol% $MgCO_3$; by XRD, Methods) had significantly less ($p < 0.001$) weight loss than the lower mol% group (16.3 – 17.45 mol% $MgCO_3$). The higher mol% group had

[1]Research School of Physics, The Australian National University, Acton, Australian Capital Territory 0200, Australia, [2]Research School of Earth Sciences, The Australian National University, Acton, Australian Capital Territory 0200, Australia, [3]Southern Seas Ecology Laboratories, School of Earth and Environmental Sciences, University of Adelaide, Adelaide, South Australia 5005, Australia, [4]National Museum of Natural History, Smithsonian Institution, Washington DC 20013, USA, [5]Takehara Fisheries Research Station, Center for Education and Research of Field Science, Hiroshima University, Minato-machi, Takehara, Hiroshima 725-0024, Japan, [6]Griffith School of Environment and Australian Rivers Institute—Coast and Estuaries, Griffith University, Brisbane, Nathan, Queensland 4111, Australia, [7]Scripps Institution of Oceanography, University of California, San Diego, La Jolla, California 92093, USA, [8]Coral Reef Ecosystems Laboratory, School of Biological Sciences, University of Queensland, Brisbane, Queensland 4072, Australia.
*e-mail: merinda.nash@anu.edu.au.

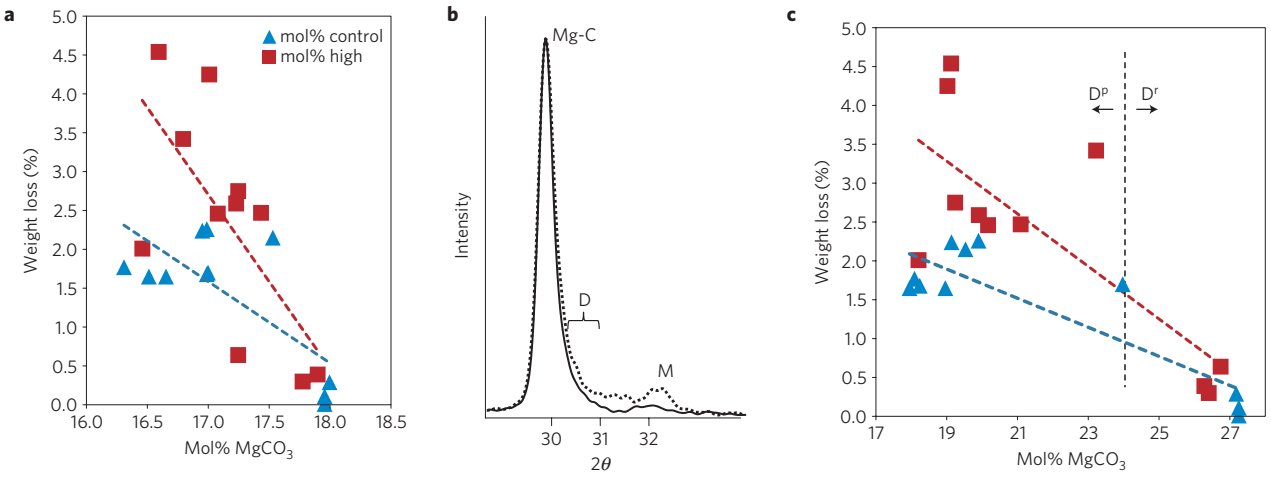

Figure 1 | Dependence of weight loss of coralline algae on composition (mol% $MgCO_3$). **a**, Weight loss versus Mg-calcite composition, showing a trend for higher weight loss with lower Mg content in both control ($R = -0.74$) and high ($R = -0.69$) CO_2 treatment samples. The slopes are significantly different (Supplementary Table S3b). The more Mg-rich CCA have the most asymmetrical Mg-calcite XRD peaks. Mg contents determined using the Mg-calcite peak position. **b**, Typical XRD scans for D^r (dotted line) and D^p CCA (solid line). Mg-C, Mg-calcite; D, dolomite range (M.C.N. *et al.*, manuscript in preparation); M, magnesite. **c**, Weight loss versus Mg-calcite composition as determined using the asymmetrical peak position (M.C.N. *et al.*, manuscript in preparation; asymm mol%; Supplementary Fig. S3). Compared with **a**, which shows the same samples, the regression has improved, with control ($R = -0.87$) and high CO_2 ($R = -0.77$). The slopes are significantly different (Supplementary Table S3b).

an average weight loss of 0.17% (s.d. 0.13) and 0.51% (s.d. 0.19), respectively, which was ~91% and 83% less than the lower mol% group (Supplementary Table S3a). This trend was also observed in a five-day *in situ* ocean acidification experiment[15]. The Mg-calcite XRD peaks for the more Mg-rich CCA demonstrated extreme asymmetry (Fig. 1b), which we discovered indicated the presence of dolomite and magnesite[4]. The less Mg-rich CCA showed only slight asymmetry and this was confirmed to represent a lesser amount of dolomite. We developed a simple technique to numerically describe this asymmetry (M.C.N. *et al.*, manuscript in preparation; Supplementary Fig. S3) and found a negative correlation between this dolomite and magnesite asymmetry and weight loss (Fig. 1c); control: $R = -0.87$ ($p = 0.01$), and high CO_2: $R = -0.77$ ($p = 0.01$; statistics summary Supplementary Table S3b). We classify the CCA with asymmetry >24 mol% $MgCO_3$ as dolomite rich (D^r) and those <24 mol% $MgCO_3$ as dolomite poor (D^p) (Methods).

Next, to understand the differences between the D^r and D^p CCA that could be constraining the dissolution, we compared the physical distribution of dolomite within the D^r and D^p CCA (scanning electron microscopy (SEM), Methods). The key difference was that only the D^r CCA had dolomite lining the regular cell spaces (Fig. 2a), whereas D^p had Mg-calcite (Fig. 2b). Both D^r and D^p CCA had cell infill commencing ~50–100 μm below the surface. In D^r CCA this cell infill could be magnesite (Fig. 2c) or dolomite, whereas in D^p CCA, cells were either left void or infilled with Mg-calcite (Fig. 2d) and infrequently, magnesite (Supplementary Fig. S4). Dolomite lining in the D^r CCA formed as rhombs and submicrometre-sized mounds (Fig. 2e–g). In both the D^p and D^r CCA the reproductive conceptacles contained dolomite (Fig. 3a,b, enlargements Supplementary Figs S5 and S6). A particularly intriguing difference in their natural dissolution process is revealed in the bottom 100 μm; the D^r CCA was visibly dense whereas that of the D^p CCA was mostly porous owing to limited cell infill (Fig. 3c,d). We used a gridded point count (Supplementary Information) to estimate the porosity for D^r CCA at 6% and D^p CCA at 65%, a figure that closely matched the tenfold difference in dissolution between the D^r and D^p CCA. We estimate that the stable dolomite reduces the reactive surface area in D^r CCA by ~45% (estimated from the point count). The net dissolution process seems to be one of selective mineral dissolution and precipitation. In the base of the D^r CCA, Mg-calcite fills cells, magnesite was absent and the dolomite rims remained intact, thus retaining density. In contrast, in the D^p CCA the cell infill and interfilament Mg-calcite had dissolved, and only the cell-lining Mg-calcite remained. It seems that the process of physical break-up in the D^r CCA occurs through the dissolution of the interfilament and cell-wall Mg-calcite until sufficient wall material has been removed for the dissolution-resistant dolomite cell cast to drop out intact (Fig. 4a,b). These dolomite cell casts are not only thermodynamically stable but also physically harder than the surrounding Mg-calcite (Fig. 4c). In the D^r CCA, alteration to mineralogy seems to commence about 500–600 μm up from the base (Supplementary Fig. S7) and similarly in the D^p CCA. Aragonite also infilled discrete cells (Supplementary Fig. S8) and replaced parts of the CCA skeleton. The common Mg-calcite cell infill in the D^p and absence from the D^r (excluding the exposed base) implies that it is unlikely that the D^p is a mid-stage in the formation of D^r CCA. Some CCA had XRD asymmetry that was between D^r and D^p; SEM revealed banding of layers with and without dolomite rims and little cell infill (Supplementary Fig. S9).

To confirm the sequence of mineral dissolution and removal we performed an etching experiment on the D^r and D^p CCA (Methods). We found no evidence of cell rim dolomite dissolution; however, dolomite seems to be removed from conceptacles (Supplementary Fig. S10). In both samples the interfilament Mg-calcite is preferentially removed followed by the cell wall Mg-calcite (Supplementary Fig. S11a–f). Freshwater experiments on dolomite limestone have demonstrated that dissolution rates of dolomite are independent of pH between 6 and 8 (ref. 16) and that water flow velocity is the strongest control on dissolution rates of calcite[17]. Indeed, pore space and permeability are the key parameters influencing skeletal breakdown in temperate coralline algae in undersaturated conditions[18]. We propose that stability of the D^r CCA is conferred by their low porosity reducing water flow velocity throughout the lower crust, thereby reducing all dissolution reaction rates[17,19] and allowing re-precipitation of Mg-calcite within cell spaces. These processes combined result in a net physical break-up to an order of magnitude less than that for D^p CCA without dolomite cell lining. The degree of this stability will be influenced by the quantity of dolomite and cell infill.

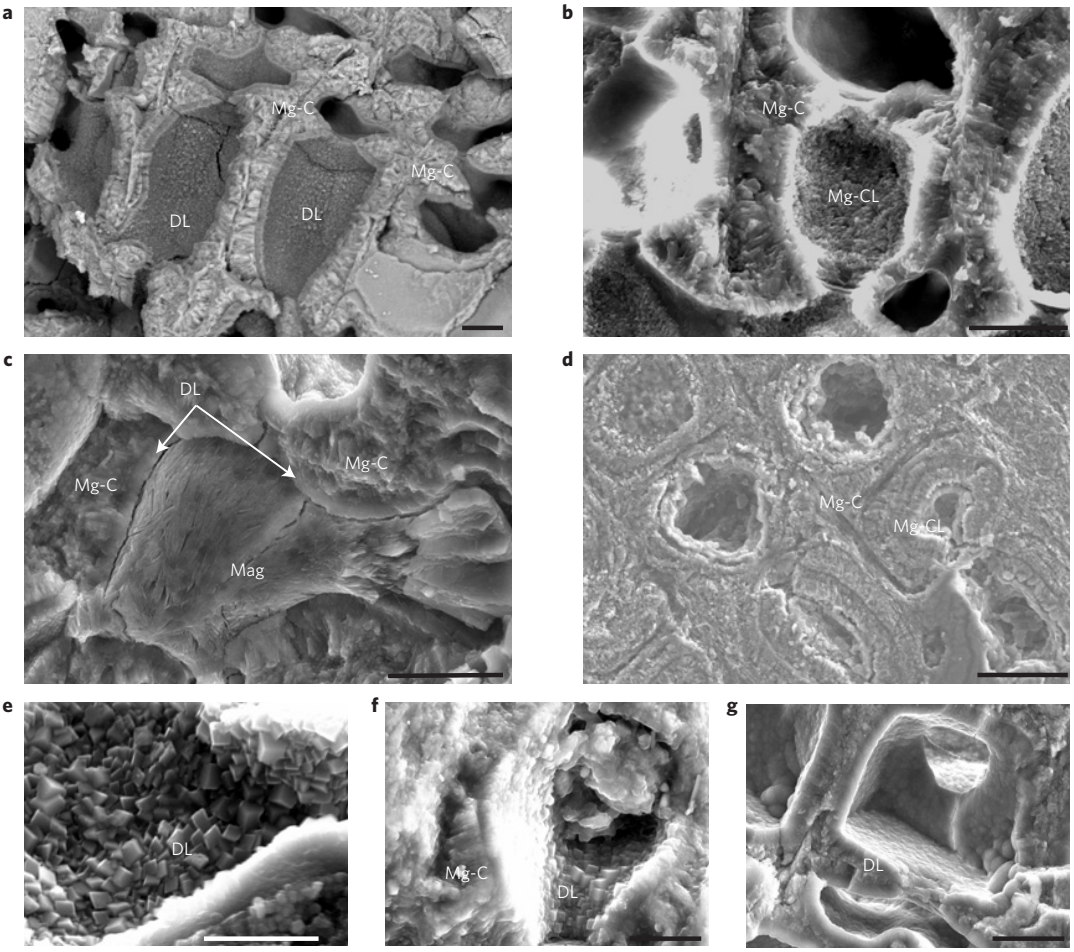

Figure 2 | Comparison of intracellular mineralization in the D^r and D^p coralline algae. a, D^r CCA (H305) has cells lined with dolomite (DL), whereas cell walls and interfilament calcified areas are composed of Mg-calcite (Mg-C). **b**, D^p CCA (H311) shows cells with an Mg-calcite lining (Mg-CL). **c**, D^r CCA (H305) has magnesite (Mag) cell infill. Dolomite lining (white arrows) forms a narrow rim between the Mg-calcite cell wall and the cell infill. **d**, D^p CCA (H56) has cell infill by concentric rings of Mg-calcite. **e**, D^r CCA (H305); close up of dolomite rhombs forming cell lining. **f**, (H305) dolomite cell infill with organic coating. **g**, CCA (H320) shows dolomite rims with dolomite submicrometre-sized mounds on the surface. Scale bars, 5 μm (**a**–**d**) and 2 μm (**e**–**g**).

The next question is how prevalent is this dolomite phenomenon? To answer this we determined the mineralogy of samples collected from multiple coral reefs from the Pacific and Caribbean. We found D^r CCA in our samples from shallow reef locations at Heron Island (southern Great Barrier Reef), Lizard Island (northern Great Barrier Reef), Okinawa (northern Pacific) and the Caribbean (Supplementary Table S5 and Figs S12 and S13). Dolomite was most commonly found in dense crusts (>3 mm) from high-energy, light environments and was absent from thin crusts growing in shaded locations. CCA skeleton in a reef front algal rim core[6] from Rodrigues (Indian Ocean) demonstrated asymmetry comparable to D^r of fresh CCA (Supplementary Table S5 and Figs S14–S16). These samples were from 35 to 80 cm and 3.2 m down core, an estimated age of 290–670 yr and 2,670 yr, respectively, indicating that this biomineralized dolomite is stable long after the organism has died. We reviewed previous studies that recorded bulk magnesium measurements higher than ~18 mol% $MgCO_3$ or XRD asymmetry (for example, refs 8,9,20) to determine whether these CCA may have had the type of dolomite mineralization we have detailed here. Every one of the six coral reefs in those studies had algal-ridge-building CCA with bulk magnesium amounts or XRD profiles that matched our assessment for D^r, five of these with magnesite, (Supplementary Tables S6a–d and Fig. S17) and included multiple species. By combining these published reports with our results we demonstrate that D^r CCA are present in the tropical Indian, Atlantic, North and South Pacific oceans (Supplementary Map S1). Dolomite was not detected in temperate samples in our study (three locations) or in the reviewed studies, suggesting that its formation may be primarily constrained by temperature. These results are in accord with evidence from the geological record for a correlation with higher temperatures and dolomite formation[5].

The final question of importance is whether these D^r CCA will continue to survive and produce dolomite under predicted future CO_2 levels. Previous studies have suggested that CCA may be susceptible to ocean acidification[14,21,22]; however, not all have found negative outcomes[23]. Crucially, none of these studies replicated the high-energy environments in which the D^r crusts form. The low dissolution rates for the D^r CCA in our experimental high-CO_2 treatment demonstrate that these CCA skeletons are unlikely to suffer annual net dissolution in this scenario. The reef front does not experience the extreme diel pH fluctuations as used in our experiment; this will probably further reduce dissolution rates and the net impact will be also be governed by biological tissue coverings, reef attachment, growth and bio-erosion[14]. The high dissolution rate for the D^p CCA is concerning as this indicates that there may be no contribution to the reef lagoon sediment from their skeletons as p_{CO_2} approaches the experimental levels of ~500–700 ppm.

Although the exact process driving dolomite formation in the CCA has yet to be determined, considering the abundance of

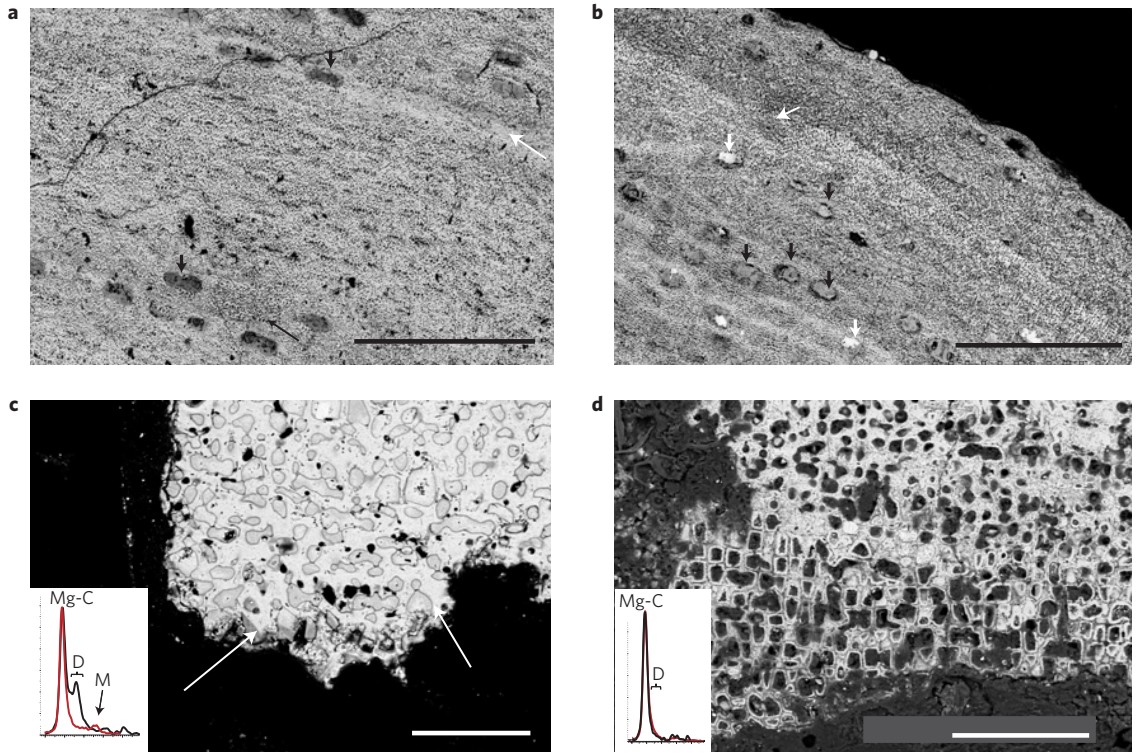

Figure 3 | Overview of D^r and D^p coralline algae with evidence of natural dissolution processes at the base exposed to sea water and corresponding XRD patterns. Both samples were living at the time of collection and were kept out of the experimental tanks as dry controls. **a**, D^r CCA—dolomite and magnesite fill the conceptacles (thick black arrows). Banding of dolomite cell infill (white arrow) and magnesite infill (thin black arrow) suggests a seasonal influence on mineralization; scale bar, 1 mm (enlargements Supplementary Figs S6 and S7). **b**, D^p CCA—dolomite (dark grey) is detected only in reproductive conceptacle spaces (black arrows), whereby some conceptacles have normal cell regrowth (narrow white arrow). Small patches of aragonite (white) infill (thick white arrows) are common; scale bar, 1 mm. **c**, D^r CCA—rims remain dolomite (white arrows) as in layers above; cell infill is now only Mg-calcite with no magnesite remaining; scale bar, 50 μm. XRD (inset) of this bottom layer (black) shows the Mg-calcite (Mg-C) peak and the separate peak for dolomite (D), and the magnesite peak (M) is absent compared to the total sample (red). **d**, D^p CCA—cell rims are Mg-calcite (light grey). Cells are empty (black) or infilled with Mg-calcite. Fluffy black material over cells is resin; scale bar, 100 μm. Mg-calcite XRD (inset) peak shows minimal dolomite asymmetry in the base layer (black), which is marginally less than for the total sample (red).

sedimentary dolomite in greenhouse epochs[5] and the evidence for an organic driver[4,24,25], it is reasonable to suggest that dolomite biomineralization is not inhibited by low saturation state. Support for this notion comes from a recent study demonstrating that dolomite can form abiotically in red algae polysaccharide solutions at starting pH of 7.7–7.9 (ref. 24). Interestingly, magnesium uptake was positively correlated with polysaccharide concentration. CCA are rich in polysaccharides[26] and light can concentrate polysaccharides at the cell perimeter of red algae[27]. In addition, dolomite formation seems to occur as a process of cell infilling in cells not in direct contact with external water conditions. Considering these studies together with our observations, it seems probable that dolomite mineralization in the CCA is not driven primarily by seawater saturation state. Rather, mineralization is probably reliant on, first, the provision of sufficiently concentrated nucleating sites (organic templates with the CCA), perhaps driven by light and temperature; the subsequent dolomite mineralization may then depend on a further set of suitable environmental conditions, possibly the key being temperature.

Although our data show D^r CCA with cell infill are not impervious to increasing dissolution under both present and higher CO_2, this distinctive dolomite intracellular calcification clearly provides substantial resistance to dissolution in comparison with predominantly Mg-calcite CCA. Laboratory experiments used to determine Mg-calcite dissolution rate data resulted in diagenetic outcomes, that is, the formation of substantial amounts of calcite (for example, ref. 10), that were not observed in our samples (Supplementary Fig. S17). This suggests that the dissolution data derived from these experiments and subsequent comparisons to aragonite may not be applicable to CCA in their natural environment. We do not ignore that reef stability may be reduced under projected future conditions; however, the stability of dolomite-enriched algal ridge coralline algae offers a positive light in a potentially gloomy future for coral reefs. Until the process and drivers of dolomite formation are understood, the biological response of CCA to higher CO_2 (and probably temperature), and therefore its ultimate contribution to reef stability, will remain uncertain.

Methods

CCA *P. onkodes* were collected for the dissolution experiment from the reef front of Heron Island in 2009 (details in ref. 4). Crusts collected had pink living surfaces and exposed bases and were broken off the reef, not dug out. Four crusts of fresh CCA were cleaned by hand of any epiphytes and loose material using a small wooden pick and brush; no chemical cleaning was applied. These crusts were broken into 25 pieces of approximately 1 cm^3. They were sun dried for two days including cleaning time, in the oven at 40 °C for 9 h and confirmed as no longer photosynthetically active, using a pulse-amplitude-modulated fluorometer. All samples were subject to an equal amount of drying time before the experiment. CCA were dry weighed to the nearest milligram, sensitivity ±0.001 g. The CCA pieces were randomly distributed between the control ($n = 3$) and treatment ($n = 3$) flow-through tanks (tank set-up, flow-through system and CO_2 control are as described in refs 15,28). Dry controls were kept and not used in the experiment to identify any changes in mineralogy due to treatment effect; the XRD results were comparable to samples from both control and treatment tanks (Supplementary Table S3a). After ten days in treatment tanks, samples were sun dried for seven days and re-weighed. All samples were subject to an equal amount of drying time after the experiment. There was no correlation between starting weight and weight lost. Dissolved inorganic carbon and alkalinity in tanks were determined as in ref. 15. A Mettler Toledo

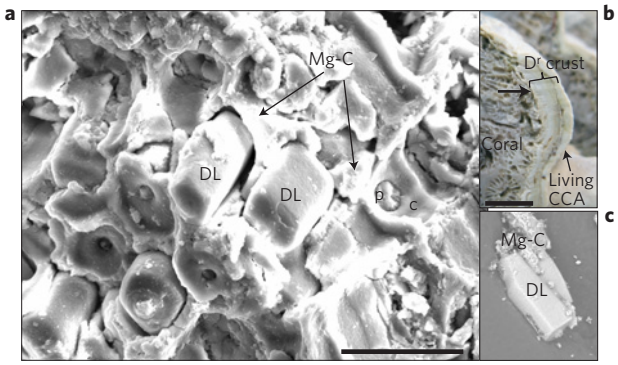

Figure 4 | D^r CCA crust on coral branch. Example of the natural break-up of the CCA crust (the surface of this 1-cm-thick crust was living at the time of collection, collected from Heron reef front 0–2 m depth). **a**, SEM of dolomite cells at the base of a D^r CCA (H601). The Mg-calcite cell wall is disintegrating, leaving the dolomite casts of the cells (DL) protruding until sufficient framework has been removed so that the cell casts drop out. p, Mg-calcite pit connector; c, cell wall interior; scale bar, 20 μm. **b**, Living coralline (H601) overgrowing coral. There is a visible gap between the CCA and the coral where the base of the CCA was exposed to sea water; wide arrow—location of SEM image in **a**; pink surface is the living coralline layer and dolomite infill starts 100–200 μm down into the crust. It is not known whether the dolomite fills in living or dead cells; scale bar, 1 cm. **c**, Lowest layer subsample (H305) after grinding in a mortar and pestle for XRD, demonstrating that dolomite casts are resistant to grinding whereas the surrounding Mg-calcite has been reduced to a submicron size.

pH meter was used for discrete pH measurements. XRD was undertaken after the completion of the experiment. XRD and SEM with energy-dispersive spectroscopy followed[4] and the dolomite range was determined as in M.C.N. *et al.* (manuscript in preparation). For classification of D^r versus D^p CCA we classify those above 24 asymm. mol% as D^r; however, we also compare XRD peak asymmetry shape to check that the dolomite asymmetry matches samples with D^r mineralogy as confirmed by SEM (as detailed in Fig. 2). Visual inspection of the XRD for the two samples just less than 24 mol% showed that the curve in the dolomite slope was less than that for samples with D^r mineralogy (see legend to Supplementary Table S5 for further discussion).

For etching, polished samples in resin were placed in a 200 ml beaker of deionized water with the pH adjusted by the addition of HNO_3 or HCl. In the first etching for 1 h, the pH ranged from 7.98–8.01; in the second etching for 6 h, the pH ranged from 7.7–7.82. The water was stirred continuously and the temperature ranged from 25 to 28 °C. To assess the mineralogy of previous studies, information on XRD and bulk magnesium was compared with that from our studies where mineralogy had also been confirmed by SEM with energy-dispersive spectroscopy.

Received 4 July 2012; accepted 31 October 2012; published online 9 December 2012

References

1. Littler, M. M. & Doty, M. S. Ecological components structuring seaward edges of Tropical Pacific reefs: Distribution, communities and productivity of Porolithon. *J. Ecol.* **63,** 117–129 (1975).
2. Adey, W. H. & Macintyre, I. G. Crustose coralline algae: A re-evaluation in the geological sciences. *Geol. Soc. Am. Bull.* **84,** 883–904 (1973).
3. Bischoff, W. D., Bishop, F. C. & Mackenzie, F. T. Biogenically produced magnesian calcite: In homogeneities in chemical and physical properties; comparison with synthetic phases. *Am. Mineral.* **68,** 1183 (1983).
4. Nash, M. C. *et al.* First discovery of dolomite and magnesite in living coralline algae and its geobiological implications. *Biogeosciences* **8,** 3331–3340 (2011).
5. Wilkinson, B. W. & Given, R. K. Secular variation in abiotic marine carbonates: Constraints on phanerozoic atmospheric carbon dioxide contents and oceanic Mg/Ca ratios. *J. Geol.* **94,** 321–333 (1986).
6. Rees, S. A., Opdyke, B. N., Wilson, P. A. & Fifield, L. K. Coral reef sedimentation on Rodrigues and the Western Indian Ocean and its impact on the carbon cycle. *Phil. Tran. R. Soc. A* **363,** 101–120 (2005).
7. Adey, W. H. Review: Coral reefs: Algal structured and mediated ecosystems in shallow, turbulent, alkaline waters. *J. Phycol.* **34,** 393–406 (1998).
8. Chave, K. E. Aspects of the biogeochemistry of magnesium 1. Calcareous marine organisms. *J. Geol.* **62,** 266–283 (1954).
9. Milliman, J. D., Gastner, M. & Muller, J. Utilization of magnesium in coralline algae. *Geol. Soc. Am. Bull.* **82,** 573–580 (1971).
10. Plummer, L. N. & Mackenzie, F. T. Predicting mineral solubility from rate data: Application to the dissolution of magnesian calcites. *Am. J. Sci.* **274,** 61–83 (1974).
11. Bischoff, W. D., Mackenzie, F. T. & Bishop, F. C. Stabilities of synthetic magnesian calcites in aqueous solution: Comparison with biogenic materials. *Geochim. Cosmochim. Acta* **51,** 1413–1423 (1987).
12. Morse, J. W., Arvidson, R. S. & Luttge, A. Calcium Carbonate formation and dissolution. *Chem. Rev.* **107,** 342–381 (2007).
13. Santos, I. R., Glud, R. N., Maher, D. & Eyre, B. D. Diel coral reef acidification driven by pore water advection in permeable carbonate sands, Heron Island, Great Barrier Reef. *Geophys. Res. Lett.* **38,** L03604 (2011).
14. Diaz-Pulido, G., Anthony, K. R. N., Kline, D. I., Dove, S. & Hoegh-Guldberg, O. Interactions between ocean acidification and warming on the mortality and dissolution of coralline algae. *J. Phycol.* **48,** 32–39 (2012).
15. Kline, D. I., Teneva, L., Schneider, K., Miard, T. & Chai, A. *et al.* A short-term *in situ* CO_2 enrichment experiment on Heron Island (GBR). *Sci. Rep.* **2,** 413 (2012).
16. Pokrovsky, O. S. & Schott, J. Kinetics and mechanism of dolomite dissolution in neutral to alkaline solutions revisited. *Am. J. Sci.* **301,** 597–626 (2001).
17. Al-Kawaz, H. A. Dissolution Rate Constant of Carbonates under Natural Environments. *Tikrit J. Pure Sci.* **15** (3), 84–90 (2010).
18. Henrich, R. & Wefer, G. Dissolution of biogenic carbonates: Effects of skeletal structure. *Mar. Geol.* **71,** 341–362 (1986).
19. Opdyke, B. N., Gust, G. & Ledwell, J. R. Mass transfer from smooth alabaster surfaces in turbulent flows. *Geophys. Res. Lett.* **14,** 1131–1134 (1987).
20. Clarke, F. W. & Wheeler, W. C. *The Inorganic Constituents of Marine Invertebrates* (USGS, 1922).
21. Kuffner, I. B., Andersson, A. J., Jokiel, P. L., Rodgers, K. S. & Mackenzie, F. T. Decreased abundance of crustose coralline algae due to ocean acidification. *Nature Geosci.* **1,** 114–117 (2008).
22. Anthony, K. R. N., Kline, D. I., Diaz-Pulido, G., Dove, S. & Hoegh-Guldberg, O. Ocean acidification causes bleaching and productivity loss in coral reef builders. *Proc. Natl Acad. Sci. USA* **105,** 17442–17446 (2008).
23. Ries, J. B., Cohen, A. L. & McCorkle, D. C. Marine calcifiers exhibit mixed responses to CO_2-induced ocean acidification. *Geology* **37,** 1131–1134 (2009).
24. Zhang, F., Xu, H., Konishi, H., Shelobolina, E. S. & Roden, E. E. Polysaccharide-catalyzed nucleation and growth of disordered dolomite: A potential precursor of sedimentary dolomite. *Am. Mineral.* **97,** 556–567 (2012).
25. Krause, S. *et al.* Microbial nucleation of Mg-rich dolomite in exopolymeric substances under anoxic modern seawater salinity: New insight into an old enigma. *Geology* **40,** 587–590 (2012).
26. Bilan, M. I. & Usov, A. I. Polysaccharides of calcareous algae and their effect on the calcification process. *Russ. J. Bioorg. Chem.* **27,** 2–16 (2001).
27. Ramus, J. The production of extracellular polysaccharide by the unicellular red algae *Porphyridium aerugineum*. *J. Phycol.* **8,** 97–111 (1972).
28. Doropoulos, C., Ward, S., Diaz-Pulido, G., Hoegh-Guldberg, O. & Mumby, P. J. Ocean acidification reduces coral recruitment by disrupting intimate larval-algal settlement interactions. *Ecol. Lett.* **15,** 338–346 (2012).

Acknowledgements

Thanks to F. Brink and the team at the ANU Centre for Advanced Microscopy for assistance with SEM work, A. Harvey for CCA samples from Victoria, L. Teneva for differential interference contrast analyses, J. Caves for field work assistance, the FOCE team and staff at Heron Island Research Centre, J. W. Lai and D. Nash for sample preparation. S. Connell for assistance with Heron experiments and J. Roberts for assistance with SEM.

Author contributions

M.C.N. and B.N.O. designed initial project; M.C.N., B.D.R. and D.I.K. carried out Heron Island experimental work and water chemistry measurements; U.T. assisted with subsequent analyses and project design. G.D-P., sample identification and design of experimental tank facilities; A.K. and W.H.A., sample collection and identification. M.C.N., U.T. and W.H.A., SEM. M.C.N. and U.T., XRD analysis. C.B., M.G. and J.P., sample collection, survey, XRD and data analyses. M.C.N. and U.T. wrote and edited the manuscript and all authors contributed.

Additional information

Supplementary information is available in the online version of the paper. Reprints and permissions information is available online at www.nature.com/reprints. Correspondence and requests for materials should be addressed to M.C.N.

Competing financial interests

The authors declare no competing financial interests.